



Published in final edited form as:

J Neuroimmune Pharmacol. 2012 September ; 7(3): 579–590. doi:10.1007/s11481-012-9357-0.

Antioxidant Sestrin-2 Redistribution to Neuronal Soma in Human Immunodeficiency Virus-Associated Neurocognitive Disorders

Virawudh Soontornniyomkij

HIV Neurobehavioral Research Program and Department of Psychiatry, School of Medicine, University of California, San Diego, La Jolla, CA, USA

Benchawanna Soontornniyomkij

HIV Neurobehavioral Research Program and Department of Psychiatry, School of Medicine, University of California, San Diego, La Jolla, CA, USA

David J. Moore

HIV Neurobehavioral Research Program and Department of Psychiatry, School of Medicine, University of California, San Diego, La Jolla, CA, USA

Ben Gouaux

HIV Neurobehavioral Research Program and Department of Psychiatry, School of Medicine, University of California, San Diego, La Jolla, CA, USA

Eliezer Masliah

HIV Neurobehavioral Research Program and Departments of Pathology and Neurosciences, School of Medicine, University of California, San Diego, La Jolla, CA, USA

Spencer Tung

Department of Pathology and Laboratory Medicine (Neuropathology), David Geffen School of Medicine, University of California, Los Angeles, Los Angeles, CA, USA

Harry V. Vinters

Departments of Pathology and Laboratory Medicine (Neuropathology) and Neurology, David Geffen School of Medicine, University of California, Los Angeles, Los Angeles, CA, USA

Igor Grant

HIV Neurobehavioral Research Program and Department of Psychiatry, School of Medicine, University of California, San Diego, La Jolla, CA, USA

Cristian L. Achim

HIV Neurobehavioral Research Program and Department of Psychiatry, School of Medicine, University of California, San Diego, La Jolla, CA, USA

Abstract

Sestrin-2 is involved in p53-dependent antioxidant defenses and in the maintenance of metabolic homeostasis. We hypothesize that sestrin-2 expression is altered in the brains of subjects diagnosed with human immunodeficiency virus (HIV)-associated neurocognitive disorders (HAND) due to neuronal oxidative stress. We studied sestrin-2 immunoreactivity in 42 isocortex sections from HIV-1-infected subjects compared to 18 age-matched non-HIV controls and 19 advanced Alzheimer's disease (AD) cases. With HIV infection, the sestrin-2 immunoreactivity pattern shifted from *neuropil* predominance (N) to *neuropil and neuronal-soma* co-dominance

Corresponding author: V. Soontornniyomkij Department of Psychiatry, School of Medicine, University of California, San Diego, 9500 Gilman Drive, La Jolla, CA 92093-0603, USA vsoontor@ucsd.edu Telephone: +1 858 822 4546, Fax: +1 858 534 4484.

Disclosure The authors declare that they have no actual or potential conflict of interest.

(NS) and *neuronal soma* predominance (S; $P < 0.0001$, Chi-square test for linear trend). Among HIV cases showing the NS or S pattern, HAND cases were preferentially associated with the S pattern ($n = 10$ of 20) compared to cognitively intact cases ($n = 1$ of 11; $P = 0.047$, Fisher's exact test). In AD brains, sestrin-2 immunoreactivity was mostly intense in the neuropil and co-localized with phospho-Tau immunoreactivity in a subset of neurofibrillary lesions. Phospho-Tau-immunoreactive neurofibrillary lesions were rare in HIV cases and their occurrence was not associated with HAND. Levels of isocortical 8-hydroxy-deoxyguanosine (marker of nucleic acid oxidation) immunoreactivity were not significantly altered in HAND cases compared to cognitively intact HIV cases. In conclusion, the sestrin-2 immunoreactivity redistribution to neuronal soma in HAND suggests unique involvement of sestrin-2 in the pathophysiology of HAND, which is different from the role of sestrin-2 in AD pathogenesis. Alternatively, the difference in sestrin-2 immunoreactivity distribution between HAND and AD may be related to different degrees of severity or stages of oxidative stress.

Keywords

Alzheimer's disease; HIV dementia; Neurofibrillary pathology; Oxidative stress; SESN2

Introduction

In the current era of highly active antiretroviral therapy (HAART), human immunodeficiency virus (HIV)-associated neurocognitive disorders (HAND), mostly in milder forms, continue to affect the clinical outcome of HIV infection, even in the setting of systemic viral suppression (Heaton et al. 2011; Nath et al. 2008). The differential susceptibility to the development and severity of HAND may be explained by individual differences in HIV variants, host genetic polymorphisms, and co-morbid factors such as chronic adverse effects of antiretroviral treatment, substance use, and systemic disorders unrelated to HIV, which may interact with each other in contributing to neural injury, specifically synaptodendritic degeneration in the context of chronic neuroinflammation and gliosis (Jayadev and Garden 2009). Accumulating evidence implicates oxidative stress in the pathophysiology of HAND (Steiner et al. 2006). Clinical studies have shown increased levels of 3-nitrotyrosine-modified proteins (nitrosative stress product), protein carbonyls (marker of protein oxidation), and 4-hydroxy-2-nonenal (produced by the oxidation of polyunsaturated fatty acids) in the cerebrospinal fluid (CSF) of HIV-infected patients who exhibited progressive neurocognitive decline (Bandaru et al. 2007; Haughey et al. 2004; Li et al. 2008; Turchan et al. 2003). In addition, in vitro studies and animal models suggest that HIV-1 proteins such as gp120, Tat, and Vpr cause neurodegeneration by inducing oxidative stress (Aksenov et al. 2001; Deshmane et al. 2009; Kruman et al. 1998; Wallace et al. 2006).

Reactive oxygen species (ROS) include free radicals (e.g. superoxide, hydroxyl, and nitric oxide) and other molecules that can lead to the generation of free radicals [e.g. hydrogen peroxide and peroxynitrite] (Lee et al. 2010a). Neurons are particularly vulnerable to oxidative damage because of their high levels of ROS generation mainly as byproducts of mitochondrial oxidative phosphorylation and relatively low levels of certain antioxidant enzymes such as catalase (Lee et al. 2010a; Lovell and Markesbery 2007). Accumulation of ROS leads to activation of the p53 transcription factor at the level of protein stability (Sablina et al. 2005). Under low-level stress p53 transcriptionally activates expression of antioxidant genes (such as sestrin-1, sestrin-2, and catalase), while upon severe chronic stress p53 induces expression of pro-oxidant and proapoptotic genes to facilitate cell death (Budanov 2011).

Both sestrin-1 and sestrin-2 play a key role in p53-dependent antioxidant defenses via regeneration of peroxiredoxins (thioredoxin-dependent peroxidases that catalyze decomposition of peroxides) from their hyperoxidized forms (Budanov et al. 2004) and through inhibition of the target of rapamycin (TOR) complex-1 anabolic pathway (Budanov and Karin 2008). Sestrin is also important in the maintenance of metabolic homeostasis and prevention of TOR-induced tissue degeneration (Lee et al. 2010b). With regard to neuronal homeostasis, a study in rodents showed that trans-synaptic activation of synaptic *N*-methyl-D-aspartate receptors augmented intrinsic antioxidant defenses by up-regulating sestrin-2 expression (Papadia et al. 2008).

The present study aimed at examining the role of sestrin-2 in the pathophysiology of HAND with respect to oxidative stress. We analyzed sestrin-2 immunoreactivity distribution in postmortem isocortex sections from a cohort of HIV-1-infected subjects compared to age-matched non-HIV controls. The isocortex sections were also immunostained for 8-hydroxydeoxyguanosine (8-OHdG), a marker of nucleic acid oxidation (Nunomura et al. 2001). Since previous reports have implicated oxidative stress in the pathogenesis of Alzheimer's disease [AD] (Lovell and Markesbery 2007; Nunomura et al. 2006; Smith et al. 2010), we included AD brain tissue sections in our analysis. We hypothesize that sestrin-2 protein expression is altered in the brains of HAND subjects due to neuronal oxidative stress.

Materials and methods

Study cohort

We assembled 42 autopsy HIV brains obtained during 1999–2007 from the California NeuroAIDS Tissue Network, which were processed according to the protocols adopted by the National NeuroAIDS Tissue Consortium, with the availability of clinical, laboratory, and neuropsychological data. These brains were primarily obtained from HIV subjects who participated in comprehensive neuropsychological testing for assessment of seven domains of functioning: information processing speed, attention/working memory, learning, recall memory, verbal fluency, abstract/executive functioning, and motor/psychomotor speed, with statistical correction for demographic variables (i.e. age, sex, ethnicity, and education), as described previously (Levine et al. 2008). The University of California, San Diego Human Research Protections Program approved the current project and all study participants provided written informed consent to participate. Written consent to autopsy was also obtained. All 42 HIV cases except H42 (Table 1) underwent comprehensive neuropsychological testing within a median of 22.7 weeks before death (interquartile range [IQR] = 24.9 weeks). Clinical diagnoses of HAND ($n = 21$) were made according to standard criteria (Antinori et al. 2007), including (with increasing severity of neurocognitive impairment) asymptomatic neurocognitive impairment (ANI, $n = 5$), mild neurocognitive disorder (MND, $n = 13$), and HIV-1-associated dementia (HAD, $n = 3$). There were 9 subjects affected by neuropsychological impairment due to other or undetermined causes (NPI-O/U) and 11 subjects who were classified as cognitively normal (Table 1).

Histories of antiretroviral treatment recorded within a median of 16.4 weeks (IQR = 21.1 weeks) prior to death were grouped into *no treatment* ($n = 13$), *non-HAART regimens* ($n = 5$), and *HAART regimens* ($n = 23$) [Table 1]. In the no-treatment group, 4 subjects had never received antiretroviral drugs (cases H10, H13, H14, and H33). The antiretroviral regimens and their durations varied markedly among HIV subjects on treatment (data not shown). As evidence has linked methamphetamine-induced neurotoxicity to oxidative stress particularly in the context of HIV infection (Silverstein et al. 2011; Yamamoto et al. 2010), we included records of lifetime methamphetamine use (combining *abuse vs. dependence* and *current vs. past* categories) in our analysis. Structured diagnostic interviews, the Psychiatric Research Interview for Substance and Mental Disorders (Hasin et al. 1996) or Composite International

Diagnostic Interview (Robins et al. 1988), were used to ascertain lifetime substance use disorders based on the Diagnostic and Statistical Manual of Mental Disorders (fourth edition). Of 38 HIV subjects evaluated for methamphetamine use, only one subject (case H6) met *current dependence* criteria and no subjects met *current abuse* criteria.

Autopsy findings in the extracranial organs were primarily consistent with acquired immune deficiency syndrome, including opportunistic infections (e.g. with cytomegalovirus, pneumocystis, cryptococcus, and aspergillus) and neoplasms (e.g. non-Hodgkin's lymphomas and Kaposi's sarcoma), and also comprised hepatitis C virus infection (in 12 of 41 HIV subjects who underwent serological testing), hepatic cirrhosis, and bronchopneumonia. Of 42 HIV brains, 19 showed no significant histopathologic changes, 4 with Alzheimer type II gliosis, 8 with parenchymal vascular lesions (e.g. lacunar infarcts and microhemorrhages), 3 with focal white matter rarefaction, 5 with microglial nodules, 1 with focal cytomegalovirus encephalitis (case H6), 1 with aspergillus meningitis and cryptococcomas (H33), and 5 focally involved by primary or secondary non-Hodgkin's lymphoma (H13, H17, H18, H37, and H41). None had evidence of HIV encephalitis (i.e. the presence of multinucleated giant cells and HIV-1 p24-immunoreactive microglia).

Non-HIV controls with no history of neurological diseases (Table 2) were obtained during 1999–2007 from the California NeuroAIDS Tissue Network (n = 9) and the University of California, Los Angeles (UCLA) Division of Neuropathology (n = 9). The neuropathologic examination of the control brains revealed no significant histopathologic changes, except for Alzheimer type II gliosis (cases C6, C7, C11, and C13), lacunar infarcts (C6 and C10), microinfarcts (C3, C7, and C8), cavernous angioma (C3), and rare microglial nodules (C14). The brains of demented patients with a neuropathologic diagnosis of definite AD according to the Consortium to Establish a Registry for Alzheimer's Disease [CERAD] (Gearing et al. 1995), with Braak stages V–VI (Alafuzoff et al. 2008), were obtained during 2001–2006 from the Mary S. Easton Center for Alzheimer's Disease Research Brain Bank at UCLA (n = 19, Table 2). The neuropathologic protocols used in evaluating autopsy AD cases were described previously (Soontornniyomkij et al. 2010a).

Included in the present immunohistochemical study for sestrin-2 and phospho-Tau (p-Tau) were 5- μ m-thick formalin-fixed paraffin-embedded tissue sections of the isocortex (all of 42 HIV cases [left mid-frontal cortex], 18 controls, and 19 AD cases) and hippocampus (all of 19 AD cases). Immunostainings for 8-OHdG and glial fibrillary acidic protein (GFAP) were performed on the isocortex sections from all of 42 HIV cases (left mid-frontal cortex) and 18 controls. In either HIV or control group, the isocortex sections showed no significant histopathologic changes on hematoxylin and eosin (H&E) staining.

Immunohistochemistry

The primary antibodies used were raised against sestrin-2 (rabbit polyclonal, #10795-1-AP, ProteinTech Group, Chicago, IL, USA, 1:200 dilution in Dako antibody diluent, DakoCytomation, Carpinteria, CA, USA), p-Tau (mouse monoclonal, clone AT8, #MN1020, Pierce Biotechnology, Rockford, IL, USA, 1:1,000), 8-OHdG (goat polyclonal, #AB5830, Millipore, Billerica, MA, USA, 1:4,000), and GFAP (rabbit polyclonal, #Z0334, DakoCytomation, 1:1,000). Tissue sections were deparaffinized with xylene and rehydrated through graded ethanol series and water. Antigen retrieval was carried out in 121°C autoclave for 20 min with 10-mM Tris/1-mM EDTA-2Na/0.05% Tween-20 buffer (pH 9) for sestrin-2 and GFAP stainings or with 10-mM sodium citrate/0.05% Tween-20 buffer (pH 6) for p-Tau staining. For 8-OHdG staining, the sections were incubated in 37°C water bath for 40 min with pre-heated proteinase K solution (10 μ g/ml in 10-mM Tris-HCl [pH 7.5]/20-mM calcium chloride/50% glycerol). The sections were treated for 30 min with 0.3% hydrogen peroxide/PBS to quench endogenous peroxidase activity and then incubated for 30

min with 2.5% normal horse serum (Vector Laboratories, Burlingame, CA, USA). Following 24 h incubation at 4°C with the primary antibody, the immunoreactivity signals were detected with the species-appropriate peroxidase-micropolymer horse anti-IgG secondary antibody (ImmPRESS™, Vector Laboratories, 40 min at room temperature) and diaminobenzidine (ImmPACT™ DAB Peroxidase Substrate, Vector Laboratories, 5 min). For sestrin-2 and p-Tau stainings, the sections were counterstained with Mayer hematoxylin (Sigma-Aldrich, St. Louis, MO, USA) for 3 min. All the sections were dehydrated through graded ethanol series, cleared in xylene, and mounted with Cytoseal 60 (Richard-Allan Scientific, Waltham, MA, USA). For the negative reagent control, the primary antibody was omitted.

Qualitative assessment of DAB immunostaining

By light microscopy brain tissue sections immunostained for sestrin-2 and p-Tau were examined independently by two investigators (V. S. and C. L. A.), who were unaware of the HIV status and other clinical data.

The density of p-Tau-immunoreactive neuropil threads on each tissue section was graded as 0 (none), 1 (barely present at ×100 magnification), 2 (easily noted at ×100 magnification), and 3 (notable with naked eye inspection), a scoring system adapted from a BrainNet Europe Consortium study (Alafuzoff et al. 2008).

Quantification of immunoreactivity

The isocortex sections immunostained with DAB were digitally scanned using a microscope slide scanner (Aperio ScanScope® GL, Vista, CA, USA) equipped with a 20× objective lens (yielding the resolution of 0.5 μm per pixel). Using the ImageScope™ software (Aperio), a square of 4,500 × 4,500 μm² was extracted from each isocortex section. The immunoreactivity signals for sestrin-2, 8-OHdG, and GFAP in HIV cases and controls were quantified by means of two-dimensional image analysis using the Image-Pro® Analyzer software (version 6.3, Media Cybernetics, Bethesda, MD, USA). Isocortex images of same size and resolution were used to outline the anatomic area of interest (AOI), i.e. the isocortical layers II–VI for sestrin-2, 8-OHdG, and GFAP and the subcortical white matter for GFAP, as previously described (Soontornniyomkij et al. 2010b). In measurement of DAB intensity within the AOI, the same setting of histogram-based RGB color segmentation was applied to all the sections for each marker. The values of immunoreactivity normalized to AOI (IR_n) were calculated from three statistical measurement values, as previously described (Soontornniyomkij et al. 2010b).

For illustration, composite digital images were obtained from the Aperio digital slides. The inset images were taken with a 40× objective lens on an Olympus BX40 microscope equipped with a Nikon Digital Sight DS-5M digital camera.

Double-label immunofluorescence

The spatial relationship between sestrin-2 and p-Tau in AD isocortex sections was evaluated by double immunofluorescent staining. Antigen retrieval was performed by autoclaving at 121°C for 20 min with 10-mM sodium citrate/0.05% Tween-20 buffer (pH 6). Following incubation for 30 min with 5% normal goat serum/PBS, the tissue sections were incubated with a mixture of sestrin-2 (1:50) and p-Tau (1:1,000) antibodies at 4°C for 24 h, and then with a mixture of Alexa Fluor 568 and Alexa Fluor 488 conjugated goat anti-rabbit and anti-mouse IgG secondary antibodies (#A-21069 and #A-11017, Invitrogen, Carlsbad, CA, USA, 1:200), respectively, at room temperature for 2 h. To quench autofluorescence, the sections were incubated with 0.3% Sudan Black B/70% ethanol (#199664, Sigma-Aldrich, 15 min at room temperature). For the negative control, the primary antibody pair was omitted. The

tissue sections were cover-slipped with a mounting medium (#P7481, Invitrogen) and qualitatively examined by DeltaVision® RT deconvolution microscopy (Applied Precision, Issaquah, WA, USA).

Statistical analysis

To determine associations among categorical proportions, the Chi-square (χ^2) test and the Fisher's exact test were used. Specifically for tables having two rows (or columns) and three or more columns (or rows), to compare proportions among groups that were arranged in a natural qualitative order, the χ^2 test for linear trend was employed by giving such groups equally spaced scores (Altman 1991). The Mann-Whitney U test was employed to compare continuous variables between two independent groups. For three independent groups, we used the Kruskal-Wallis (KW) test followed by the Dunn's post hoc test. The Spearman's rank correlation (ρ) test was employed to evaluate the linear relationship between two continuous variables. The GraphPad InStat 3 for Macintosh software (GraphPad Software, La Jolla, CA, USA) was used to perform all statistical analysis. All P values calculated were 2-tailed and considered statistically significant at a threshold of $P < 0.05$.

Results

Cohort characteristics

The age at death distribution of HIV, control, and AD subjects is shown in Tables 1 and 2 (median = 45.0, 47.5, and 85.0 years; IQR = 13.0, 32.5, and 12.5 years; $n = 42, 18,$ and $19,$ respectively). No significant difference in age was found between HIV and control groups ($P = 0.81,$ U test). The postmortem intervals among HIV, control, and AD brains were not significantly different (median = 12, 15, and 16 h; IQR = 12, 12, and 14 h; $n = 41, 17,$ and $19,$ respectively; $P = 0.45,$ KW test). When only HIV and control brains were compared, the apparent difference in postmortem intervals did not reach statistical significance ($P = 0.59,$ U test).

GFAP immunoreactivity in HIV cases and controls

Although the isocortex sections of both HIV cases and controls showed no significant histopathologic changes on H&E staining, we used GFAP immunoreactivity to indicate the presence of subtle remote parenchymal injury (Sofroniew and Vinters 2010). Using quantitative image analysis, the GFAP IRn in the gray matter was 3.1-fold higher in HIV cases than that in controls (median = 0.31 and 0.10, IQR = 0.30 and 0.18, $n = 42$ and $18,$ respectively; $P = 0.008,$ U test), as was the GFAP IRn (3.9-fold) in the subcortical white matter (median = 0.97 and 0.25, IQR = 0.70 and 0.29, respectively; $P < 0.0001,$ U test).

Sestrin-2 immunoreactivity in HIV cases and controls

By qualitative assessment on light microscopy, we observed a distinct variation in sestrin-2 immunoreactivity in the isocortex of HIV cases and controls, which was classifiable into three patterns (Fig. 1a, b and c): *neuropil* predominance (N), *neuropil and neuronal-soma* co-dominance (NS), and *neuronal-soma* predominance (S). In other words, the sestrin-2 immunoreactivity became less intense in the neuropil and relatively more prominent in the neuronal soma as it shifted from the N pattern through the NS pattern to the S pattern. In the subcortical white matter, some astrocytes and microglia were immunoreactive for sestrin-2.

To validate the qualitative assessment of sestrin-2 immunoreactivity, we performed quantitative image analysis. We found a significant difference in the sestrin-2 IRn among the 3 patterns (N, NS, and S; median = 15.17, 3.18, and 0.21; IQR = 11.57, 6.15, and 0.21; $n = 15, 30,$ and $15,$ respectively; $P < 0.0001,$ KW test) and on Dunn's post hoc analysis

between each pair of sestrin-2 immunoreactivity patterns ($N > NS$, $P < 0.05$; $N > S$, $P < 0.001$; and $NS > S$, $P < 0.001$).

Among all of HIV cases and controls, there was no significant linear correlation between the sestrin-2 IRn and age at death ($\rho = 0.02$, $P = 0.89$, $n = 60$), nor was there between the sestrin-2 IRn and postmortem interval ($\rho = 0.10$, $P = 0.47$, $n = 58$).

HIV status predicted sestrin-2 immunoreactivity preference for neuronal soma

On analysis of sestrin-2 immunoreactivity in the isocortex, HIV cases showed a significant linear trend toward the S pattern compared to controls ($P < 0.0001$, χ^2 test for linear trend, Fig. 2a). Only 1 in 18 controls exhibited the S pattern and only 2 of 42 HIV cases revealed the N pattern. In other words, the sestrin-2 immunoreactivity shifted from the N pattern in controls to the NS and S patterns in HIV cases. This was supported by the finding of lower sestrin-2 IRn in HIV cases compared to that in controls (median = 1.26 and 9.42, IQR = 3.78 and 11.73, $n = 42$ and 18, respectively; $P < 0.0001$, U test).

Sestrin-2 immunoreactivity preference for neuronal soma in HAND

Because there were only two HIV cases that showed the N pattern of sestrin-2 immunoreactivity (Table 1), we excluded them from categorical association analysis. Among HIV cases with the NS or S pattern, those with HAND (i.e. ANI, MND, or HAD) were preferentially associated with the S pattern (10 of 20 cases) compared to cognitively intact cases (1 of 11 cases) [$P = 0.047$, Fisher's exact test, Fig. 2b]. This was supported by the finding of lower sestrin-2 IRn in HAND cases compared to that in HIV cases with normal cognition (median = 0.70 and 3.13, IQR = 2.82 and 9.81, $n = 20$ and 11, respectively; $P = 0.04$, U test).

Among HIV cases with the NS or S pattern, there was also a significant linear trend toward the S pattern with increasing severity of neurocognitive impairment ($P = 0.046$, χ^2 test for linear trend): normal cognition (1 of 11 cases), ANI (2 of 5 cases), MND (7 of 12 cases), and HAD (1 of 3 cases). In contrast, HIV cases with NPI-O/U showed no significant association with the S pattern (2 of 8 cases) compared to those subjects with normal cognition (1 of 11 cases) [$P = 0.55$, Fisher's exact test].

Effect of methamphetamine use

Among HIV cases with the NS or S pattern of sestrin-2 immunoreactivity, those subjects with lifetime methamphetamine use were not significantly associated with the S pattern (6 of 17 cases) compared to those without methamphetamine use (8 of 20 cases) [$P = 1.0$, Fisher's exact test]. No significant difference in the sestrin-2 IRn was observed between HIV cases with and without lifetime methamphetamine use (median = 0.72 and 1.16, IQR = 2.43 and 2.76, $n = 17$ and 20, respectively; $P = 0.80$, U test).

Effect of antiretroviral treatment

Among HIV cases with the NS or S pattern of sestrin-2 immunoreactivity, there was no significant association between antiretroviral treatment and the S pattern ($P = 0.27$, Fisher's exact test). Similarly, the apparently lower sestrin-2 IRn in HIV cases on antiretroviral treatment compared to that in HIV cases without antiretroviral treatment did not reach statistical significance (median = 1.13 and 1.42, IQR = 4.16 and 2.44, $n = 27$ and 12, respectively; $P = 0.82$, U test).

Sestrin-2 immunoreactivity in AD cases

In the isocortex and hippocampus of all AD cases, sestrin-2 immunoreactivity was in most instances intense in the neuropil without significant diffuse labeling of neuronal soma. Notably, in 18 of 19 AD brains, there were sestrin-2-immunoreactive lesions reminiscent of cytoskeletal abnormalities associated with AD, including neurofibrillary tangles and plaque-associated dystrophic neurites, of varying density in either isocortex or hippocampus or both (Table 2). In comparison to p-Tau immunoreactivity on the adjacent tissue sections, the density of sestrin-2-immunoreactive neurofibrillary tangles and dystrophic neurites was much lower than that of p-Tau (Fig. 3a and b). Double-label immunofluorescence confirmed that only a subset of p-Tau-immunoreactive neurofibrillary lesions were positive for sestrin-2 (Fig. 3c, d and e).

In contrast, no sestrin-2-immunoreactive neurofibrillary lesions were observed in any of HIV cases and controls, which was in agreement with the finding that only 9 of 42 HIV cases and 7 of 18 controls showed p-Tau immunoreactive neuropil threads in the isocortex (Tables 1 and 2, respectively) and their density was very low. The presence of p-Tau-immunoreactive lesions was not significantly associated with the HIV status ($P=0.21$, Fisher's exact test) or (in the HIV group) with HAND compared to normal cognition ($P=1.0$, Fisher's exact test).

Neuronal 8-OHdG immunoreactivity

In isocortex sections of HIV cases and controls, neuronal 8-OHdG immunoreactivity was prominent in the soma (both nucleus and cytoplasm) and apical dendrites (Fig. 4a and b), which was consistent with the fact that anti-8-OHdG antibody used in the present study recognized both 8-OHdG in DNA and 8-hydroxy-guanosine in RNA (according to the data sheet supplied by the manufacturer). On quantitative analysis, no significant difference in the isocortical 8-OHdG IRn was found between HIV cases and controls (median = 0.44 and 0.31, IQR = 0.98 and 1.33, $n=42$ and 18, respectively; $P=0.47$, U test). In the HIV group, the 8-OHdG IRn in those cases with normal cognition was not significantly different from that in HAND cases (median = 0.71 and 0.45, IQR = 0.92 and 0.99, $n=11$ and 21, respectively; $P=0.53$, U test).

Discussion

Sestrin-2 has been shown to play a key role in p53-dependent antioxidant defenses (Budanov and Karin 2008; Budanov et al. 2004). In the present study, we investigated whether sestrin-2 was involved in the pathophysiology of HAND. We found that HIV cases displayed sestrin-2 immunoreactivity preference toward neuronal soma, whereas controls showed preference for neuropil. HIV cases exhibited more prominent severity of subtle remote parenchymal injury as measured by GFAP immunoreactivity (Sofroniew and Vinters 2010) compared to controls. Furthermore, HAND cases with increasing severity of cognitive impairment were associated with the sestrin-2 immunoreactivity preference for neuronal soma compared to cognitively intact HIV cases. This sestrin-2 association appeared relatively specific to HAND as it was not observed with neurocognitive impairment unrelated to HIV infection, lifetime methamphetamine use, or antiretroviral treatment.

Our interpretation is that sestrin-2 immunoreactivity preference for neuronal soma is indicative of the response to oxidative stress affecting neurons in the context of HIV infection (Budanov et al. 2002); nonetheless, other cellular antioxidant pathways might also be involved (Budanov 2011) and these antioxidant defenses might not provide adequate protection against oxidative stress in the brains of HAND subjects. The present study suggests that oxidative stress is involved in the pathophysiology of HAND. In agreement

with our autopsy study, several clinical studies showed elevated CSF levels of molecular products of oxidative/nitrosative stress in HIV subjects with progressive cognitive impairment (Haughey et al. 2004; Li et al. 2008; Turchan et al. 2003).

In contrast to HAND brains, sestrin-2 immunoreactivity in advanced AD brains in our study was intense in the neuropil (without significant diffuse labeling of neuronal soma) and was co-localized with p-Tau immunoreactivity in a subset of neurofibrillary lesions. In agreement with our study, antibodies to other cellular antioxidant proteins, such as Cu/Zn and Mn superoxide dismutases and catalase, were shown by Pappolla et al. (1992) to mark a subset of neurofibrillary lesions in AD brains but not tangle-free neurons in AD or control brains, although the findings of a similar study by Furuta et al. (1995) were somewhat different. The p-Tau-immunoreactive neurofibrillary lesions were rare in HIV cases and their occurrence was not significantly associated with HAND. In a previous study by Nunomura et al. (2001), levels of 8-OHdG immunoreactivity in hippocampal neurons were increased in AD cases compared to age-matched non-demented controls. In our study, levels of isocortical 8-OHdG immunoreactivity were not significantly altered in HAND cases compared to cognitively intact HIV cases. In summary, the differences in immunohistologic patterns between HAND and AD suggest that these two cognitive syndromes are mediated by different mechanistic cascades although having oxidative stress in common at some point. Based on the extent of p-Tau-immunoreactive neurofibrillary pathology in the present study, AD brains (Braak stages V–VI) were in much more advanced stages of neurodegeneration than HAND brains.

To reflect the circumstances in the current era of HAART where HIV encephalitis is disappearing, we did not include cases with pathologic evidence of HIV encephalitis in the present study. However, antiretroviral agents targeting either HIV-1 protease or reverse transcriptase included in HAART regimens may have no impact on the production of HIV-1 regulatory proteins such as Tat and Vpr once proviral DNA has been integrated in infected neuroglial cells (Nath and Hersh 2005; Steiner et al. 2006). Even in the absence of productive HIV replication in the brain, HIV-1 regulatory proteins may be able to disturb neuronal homeostasis as long as the virus is sequestered in perivascular microglia/macrophages (Nath and Hersh 2005). These HIV-1 proteins may predispose the brains of HIV subjects to oxidative stress and thereby synaptodendritic degeneration (Aksenov et al. 2001; Deshmane et al. 2009; Kruman et al. 1998; Wallace et al. 2006). In cultured embryonic rat hippocampal neurons, HIV-1 Tat induced neuronal apoptosis by a mechanism involving the generation of ROS (Kruman et al. 1998). HIV-1 Vpr in microglia was also shown to induce the mitochondrial production of ROS (Deshmane et al. 2009).

Adverse effects of HAART may contribute to oxidative stress. Nucleoside reverse transcriptase inhibitors (NRTI, e.g. didanosine, stavudine, and zalcitabine) can induce mitochondrial dysfunction, resulting in oxidative stress and neuronal injury (Schweinsburg et al. 2005; Valcour and Shiramizu 2004). For instance, an in vitro study showed that zalcitabine at concentrations achievable in the CSF of HIV subjects induced oxidative stress in synaptosomes and isolated mitochondria (Opii et al. 2007). The combination of zidovudine (an NRTI) and indinavir (a protease inhibitor) was shown in immortalized human brain capillary endothelial (hCMEC/D3) cells to induce mitochondrial dysfunction, ROS production, oxidative stress, and apoptosis (Manda et al. 2011). However, in our study there was no significant association between antiretroviral treatment and sestrin-2 immunoreactivity preference for neuronal soma. This may be explained by the heterogeneous nature of data regarding the antiretroviral regimens and durations, which precludes an examination into the possible role of individual antiretroviral classes.

Methamphetamine has been documented to impair mitochondrial function and induce oxidative stress in dopaminergic and serotonergic nerve terminals, neuronal soma in the prefrontal cortex and hippocampus, and blood-brain barrier endothelial cells; additionally, this methamphetamine-mediated neurotoxicity is augmented by HIV-1 Tat (Silverstein et al. 2011; Yamamoto et al. 2010; Zhang et al. 2009). Nonetheless, we found no significant association between the sestrin-2 immunoreactivity preference for neuronal soma and lifetime methamphetamine use in HIV subjects. This unexpected finding may be explained by the fact that in our analysis we combined different categories of methamphetamine use (i.e. *abuse vs. dependence* and *past vs. current*), which may be associated with differential neurotoxic effects, into a single category of lifetime methamphetamine use due to the sample size issue. Moreover, only one of 38 HIV subjects evaluated for methamphetamine use met *current dependence* criteria.

In conclusion, the sestrin-2 immunoreactivity redistribution to neuronal soma in HAND suggests unique involvement of sestrin-2 in the pathophysiology of HAND, which is different from the role of sestrin-2 in AD pathogenesis. Alternatively, the difference in sestrin-2 immunoreactivity distribution between HAND and AD may be related to different degrees of severity or stages of oxidative stress. To validate our autopsy findings of sestrin-2 protein expression in the context of HIV infection, future studies can be conducted in other neurodegenerative diseases potentially associated with oxidative stress such as Parkinson's disease (Navarro et al. 2009), animal models of HIV-1 neuropathogenesis (e.g. gp120- or inducible Tat-transgenic mice and simian models), as well as in human neuronal cultures exposed to HIV-1 conditioned medium or hydrogen peroxide. CSF biomarkers such as HIV RNA and monocyte chemoattractant protein-1 levels that were found to correlate with HAND in the pre-HAART era have become less useful in identifying individuals affected by HAND in the HAART era (McArthur et al. 2005). To investigate whether sestrin-2 can be used as a surrogate biomarker of HAND, it will be of interest to measure sestrin-2 protein levels in CSF of HIV subjects in relation to their neurocognitive status, as it has been pursued for molecular products of oxidative/nitrosative stress (Bandaru et al. 2007; Haughey et al. 2004; Li et al. 2008; Turchan et al. 2003). Elevation of endogenous antioxidant protein levels in CSF may identify patients who are at greater risk of developing HAND and thereby would benefit from neuroprotective antioxidant therapy.

Acknowledgments

This work was supported in part by the Don & Marilyn Short Fellowship in Parkinson's Disease (to V. S.) and the United States National Institutes of Health grants R25 MH81482 (to V. S.), P50 DA26306 and R03 DA27513 (to V. S., B. S., and C. L. A.), P30 MH62512 and U01 MH83506 (to C. L. A.), R24 MH59745 (to D. J. M.), and P50 AG16570 and U01 AI35040 (S. T. and H. V. V.). DeltaVision[®] RT deconvolution microscopy was supported by the University of California, San Diego Neuroscience Microscopy Shared Facility grant P30 NS047101.

References

- Aksenov MY, Hasselrot U, Bansal AK, et al. Oxidative damage induced by the injection of HIV-1 Tat protein in the rat striatum. *Neurosci Lett*. 2001; 305:5–8. [PubMed: 11356294]
- Alafuzoff I, Arzberger T, Al-Sarraj S, et al. Staging of neurofibrillary pathology in Alzheimer's disease: a study of the BrainNet Europe Consortium. *Brain Pathol*. 2008; 18:484–496. [PubMed: 18371174]
- Altman, DG. Comparing groups - categorical data. In: *Practical statistics for medical research*. 1st edn.. Chapman and Hall; London: 1991. p. 261-265.
- Antinori A, Arendt G, Becker JT, et al. Updated research nosology for HIV-associated neurocognitive disorders. *Neurology*. 2007; 69:1789–1799. [PubMed: 17914061]

- Bandaru VV, McArthur JC, Sacktor N, Cutler RG, Knapp EL, Mattson MP, Haughey NJ. Associative and predictive biomarkers of dementia in HIV-1-infected patients. *Neurology*. 2007; 68:1481–1487. [PubMed: 17470750]
- Budanov AV. Stress-responsive sestrins link p53 with redox regulation and mammalian target of rapamycin signaling. *Antioxid Redox Signal*. 2011; 15:1679–1690. [PubMed: 20712410]
- Budanov AV, Karin M. p53 target genes sestrin1 and sestrin2 connect genotoxic stress and mTOR signaling. *Cell*. 2008; 134:451–460. [PubMed: 18692468]
- Budanov AV, Sablina AA, Feinstein E, Koonin EV, Chumakov PM. Regeneration of peroxiredoxins by p53-regulated sestrins, homologs of bacterial AhpD. *Science*. 2004; 304(5670):596–600. [PubMed: 15105503]
- Budanov AV, Shoshani T, Faerman A, et al. Identification of a novel stress-responsive gene Hi95 involved in regulation of cell viability. *Oncogene*. 2002; 21:6017–6031. [PubMed: 12203114]
- Deshmane SL, Mukerjee R, Fan S, et al. Activation of the oxidative stress pathway by HIV-1 Vpr leads to induction of hypoxia-inducible factor 1alpha expression. *J Biol Chem*. 2009; 284:11364–11373. [PubMed: 19204000]
- Furuta A, Price DL, Pardo CA, Troncoso JC, Xu ZS, Taniguchi N, Martin LJ. Localization of superoxide dismutases in Alzheimer's disease and Down's syndrome neocortex and hippocampus. *Am J Pathol*. 1995; 146:357–367. [PubMed: 7856748]
- Gearing M, Mirra SS, Hedreen JC, Sumi SM, Hansen LA, Heyman A. The Consortium to Establish a Registry for Alzheimer's Disease (CERAD). Part X. Neuropathology confirmation of the clinical diagnosis of Alzheimer's disease. *Neurology*. 1995; 45:461–466. [PubMed: 7898697]
- Hasin DS, Trautman KD, Miele GM, Samet S, Smith M, Endicott J. Psychiatric Research Interview for Substance and Mental Disorders (PRISM): reliability for substance abusers. *Am J Psychiatry*. 1996; 153:1195–1201. [PubMed: 8780425]
- Haughey NJ, Cutler RG, Tamara A, et al. Perturbation of sphingolipid metabolism and ceramide production in HIV-dementia. *Ann Neurol*. 2004; 55:257–267. [PubMed: 14755730]
- Heaton RK, Franklin DR, Ellis RJ, et al. HIV-associated neurocognitive disorders before and during the era of combination antiretroviral therapy: differences in rates, nature, and predictors. *J Neurovirol*. 2011; 17:3–16. [PubMed: 21174240]
- Jayadev S, Garden GA. Host and viral factors influencing the pathogenesis of HIV-associated neurocognitive disorders. *J Neuroimmune Pharmacol*. 2009; 4:175–189. [PubMed: 19373562]
- Kruman II, Nath A, Mattson MP. HIV-1 protein Tat induces apoptosis of hippocampal neurons by a mechanism involving caspase activation, calcium overload, and oxidative stress. *Exp Neurol*. 1998; 154:276–288. [PubMed: 9878167]
- Lee HP, Zhu X, Casadesus G, et al. Antioxidant approaches for the treatment of Alzheimer's disease. *Expert Rev Neurother*. 2010a; 10:1201–1208. [PubMed: 20586698]
- Lee JH, Budanov AV, Park EJ, et al. Sestrin as a feedback inhibitor of TOR that prevents age-related pathologies. *Science*. 2010b; 327(5970):1223–1228. [PubMed: 20203043]
- Levine AJ, Hinkin CH, Ando K, et al. An exploratory study of long-term neurocognitive outcomes following recovery from opportunistic brain infections in HIV+ adults. *J Clin Exp Neuropsychol*. 2008; 30:836–843. [PubMed: 18608693]
- Li W, Malpica-Llanos TM, Gundry R, Cotter RJ, Sacktor N, McArthur J, Nath A. Nitrosative stress with HIV dementia causes decreased L-prostaglandin D synthase activity. *Neurology*. 2008; 70:1753–1762. [PubMed: 18077799]
- Lovell MA, Markesbery WR. Oxidative damage in mild cognitive impairment and early Alzheimer's disease. *J Neurosci Res*. 2007; 85:3036–3040. [PubMed: 17510979]
- Manda KR, Banerjee A, Banks WA, Ercal N. Highly active antiretroviral therapy drug combination induces oxidative stress and mitochondrial dysfunction in immortalized human blood-brain barrier endothelial cells. *Free Radic Biol Med*. 2011; 50:801–810. [PubMed: 21193030]
- McArthur JC, Brew BJ, Nath A. Neurological complications of HIV infection. *Lancet Neurol*. 2005; 4:543–555. [PubMed: 16109361]
- Nath A, Hersh LB. Tat and amyloid: multiple interactions. *AIDS*. 2005; 19:203–204. [PubMed: 15668546]

- Nath A, Schiess N, Venkatesan A, Rumbaugh J, Sacktor N, McArthur J. Evolution of HIV dementia with HIV infection. *Int Rev Psychiatry*. 2008; 20:25–31. [PubMed: 18240060]
- Navarro A, Boveris A, Báñez MJ, Sánchez-Pino MJ, Gómez C, Muntané G, Ferrer I. Human brain cortex: mitochondrial oxidative damage and adaptive response in Parkinson disease and in dementia with Lewy bodies. *Free Radic Biol Med*. 2009; 46:1574–1580. [PubMed: 19298851]
- Nunomura A, Castellani RJ, Zhu X, Moreira PI, Perry G, Smith MA. Involvement of oxidative stress in Alzheimer disease. *J Neuropathol Exp Neurol*. 2006; 65:631–641. [PubMed: 16825950]
- Nunomura A, Perry G, Aliev G, et al. Oxidative damage is the earliest event in Alzheimer disease. *J Neuropathol Exp Neurol*. 2001; 60:759–767. [PubMed: 11487050]
- Opii WO, Sultana R, Abdul HM, Ansari MA, Nath A, Butterfield DA. Oxidative stress and toxicity induced by the nucleoside reverse transcriptase inhibitor (NRTI)--2',3'-dideoxycytidine (ddC): relevance to HIV-dementia. *Exp Neurol*. 2007; 204:29–38. [PubMed: 17069802]
- Papadia S, Soriano FX, Léveillé F, et al. Synaptic NMDA receptor activity boosts intrinsic antioxidant defenses. *Nat Neurosci*. 2008; 11:476–487. [PubMed: 18344994]
- Pappolla MA, Omar RA, Kim KS, Robakis NK. Immunohistochemical evidence of oxidative [corrected] stress in Alzheimer's disease. *Am J Pathol*. 1992; 140:621–628. [PubMed: 1372157]
- Robins LN, Wing J, Wittchen HU, et al. The Composite International Diagnostic Interview. An epidemiologic instrument suitable for use in conjunction with different diagnostic systems and in different cultures. *Arch Gen Psychiatry*. 1988; 45:1069–1077. [PubMed: 2848472]
- Sablina AA, Budanov AV, Ilyinskaya GV, Agapova LS, Kravchenko JE, Chumakov PM. The antioxidant function of the p53 tumor suppressor. *Nat Med*. 2005; 11:1306–1313. [PubMed: 16286925]
- Schweinsburg BC, Taylor MJ, Alhassoon OM, et al. Brain mitochondrial injury in human immunodeficiency virus-seropositive (HIV+) individuals taking nucleoside reverse transcriptase inhibitors. *J Neurovirol*. 2005; 11:356–364. [PubMed: 16206458]
- Silverstein PS, Shah A, Gupte R, Liu X, Piepho RW, Kumar S, Kumar A. Methamphetamine toxicity and its implications during HIV-1 infection. *J Neurovirol*. 2011; 17:401–415. [PubMed: 21786077]
- Smith MA, Zhu X, Tabaton M, et al. Increased iron and free radical generation in preclinical Alzheimer disease and mild cognitive impairment. *J Alzheimers Dis*. 2010; 19:363–372. [PubMed: 20061651]
- Sofroniew MV, Vinters HV. Astrocytes: biology and pathology. *Acta Neuropathol*. 2010; 119:7–35. [PubMed: 20012068]
- Soontornniyomkij V, Lynch MD, Mermash S, Pomakian J, Badkoobehi H, Clare R, Vinters HV. Cerebral microinfarcts associated with severe cerebral beta-amyloid angiopathy. *Brain Pathol*. 2010a; 20:459–467. [PubMed: 19725828]
- Soontornniyomkij V, Risbrough VB, Young JW, Wallace CK, Soontornniyomkij B, Jeste DV, Achim CL. Short-term recognition memory impairment is associated with decreased expression of FK506 binding protein 51 in the aged mouse brain. *Age (Dordr)*. 2010b; 32:309–322. [PubMed: 20422297]
- Steiner J, Haughey N, Li W, et al. Oxidative stress and therapeutic approaches in HIV dementia. *Antioxid Redox Signal*. 2006; 8:2089–2100. [PubMed: 17034352]
- Turchan J, Pocernich CB, Gairola C. Oxidative stress in HIV demented patients and protection ex vivo with novel antioxidants. *Neurology*. 2003; 60:307–314. [PubMed: 12552050]
- Valcour V, Shiramizu B. HIV-associated dementia, mitochondrial dysfunction, and oxidative stress. *Mitochondrion*. 2004; 4:119–129. [PubMed: 16120377]
- Wallace DR, Dodson S, Nath A, Booze RM. Estrogen attenuates gp120- and tat1-72-induced oxidative stress and prevents loss of dopamine transporter function. *Synapse*. 2006; 59:51–60. [PubMed: 16237680]
- Yamamoto BK, Moszczynska A, Gudelsky GA. Amphetamine toxicities: classical and emerging mechanisms. *Ann N Y Acad Sci*. 2010; 1187:101–121. [PubMed: 20201848]
- Zhang X, Banerjee A, Banks WA, Ercal N. N-Acetylcysteine amide protects against methamphetamine-induced oxidative stress and neurotoxicity in immortalized human brain endothelial cells. *Brain Res*. 2009; 1275:87–95. [PubMed: 19374890]

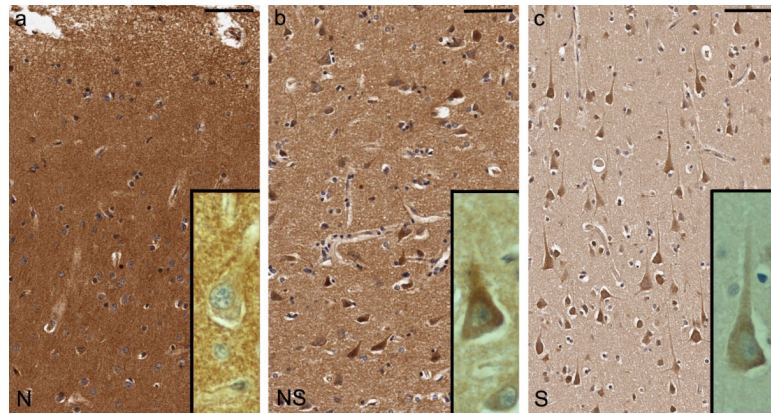


Fig. 1. Sestrin-2 immunoreactivity in the isocortex of subjects with human immunodeficiency virus (HIV) infection and non-HIV controls is classified into three patterns: **(a)** *neuropil* predominance (N, case C6), **(b)** *neuropil and neuronal-soma* co-dominance (NS, case H7), and **(c)** *neuronal-soma* predominance (S, case H35). In other words, the sestrin-2 immunoreactivity becomes less intense in the neuropil and relatively more prominent in the neuronal soma as it shifts from the N pattern through the NS pattern to the S pattern. Bars: 75 μ m (**a**, **b**, **c**)

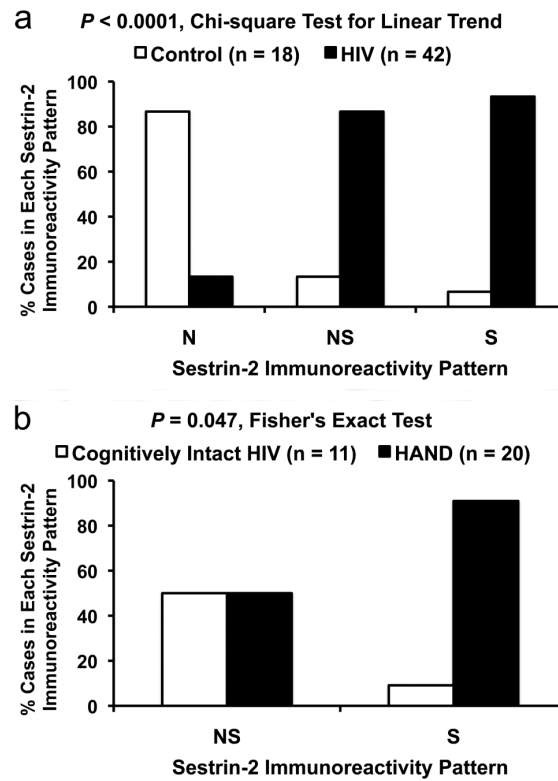


Fig. 2. Sestrin-2 immunoreactivity in the isocortex of subjects with human immunodeficiency virus (HIV) infection and non-HIV controls is classified into three patterns: *neuropil* predominance (N), *neuropil and neuronal-soma* co-dominance (NS), and *neuronal-soma* predominance (S). **(a)** HIV cases show a significant linear trend toward the S pattern compared to controls. **(b)** Among HIV cases showing the NS or S pattern, those subjects diagnosed with HIV-associated neurocognitive disorder (HAND) are preferentially associated with the S pattern compared to cognitively intact HIV subjects

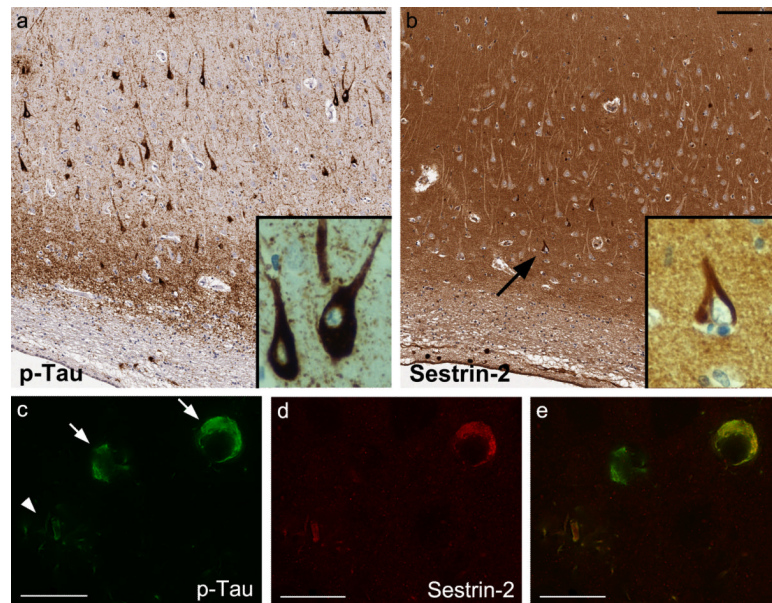


Fig. 3. In Alzheimer's disease brains, the neuropil is intensely immunoreactive for sestrin-2 and a subset of phospho-Tau (p-Tau)-immunoreactive neurofibrillary lesions are marked with sestrin-2. **(a, b)** Adjacent right hippocampal CA1 sections (case A1), bars: 150 μm . **(c, d, e)** Double-label immunofluorescence of the right mid-frontal section (case A9) reveals neurofibrillary tangles in two neurons (arrows) and plaque-associated dystrophic neurites (arrowhead), bars: 25 μm . Co-localization between p-Tau and sestrin-2 **(e, merged image)** is shown in the upper neuron and in the dystrophic neurites

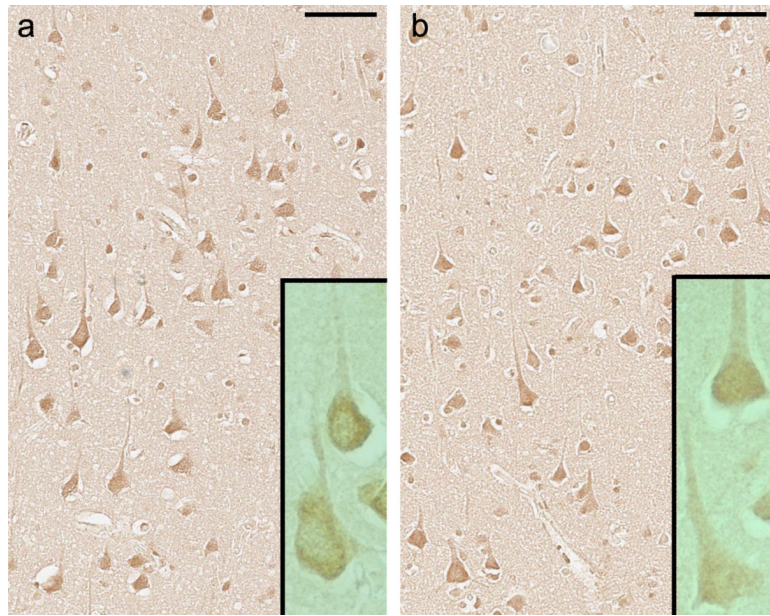


Fig. 4. Neuronal 8-hydroxy-deoxyguanosine (8-OHdG) immunoreactivity in the left mid-frontal cortex of subjects with human immunodeficiency virus infection. No significant difference in 8-OHdG immunoreactivity is observed between (a) a subject with normal cognition (case H39) and (b) a subject diagnosed with mild neurocognitive disorder (case H40), bars: 75 μ m

Table 1

Autopsy HIV cases

Case	Sestrin-2 pattern ^a	p-Tau grade ^b	Age	Sex	PMI (h)	NC Dx ^c	ARV Rx	METH
H1	N	0	55	M	24	NPI-O/U	HAART	-
H2	N	1	46	M	18	MND	No	n/a
H3	NS	0	45	M	5	NPI-O/U	HAART	+
H4	NS	0	33	M	13	MND	HAART	+
H5	NS	0	55	M	120	Normal	HAART	+
H6	NS	0	46	M	24	Normal	HAART	+
H7	NS	1	41	M	64	Normal	No	-
H8	NS	0	46	M	5	MND	No	-
H9	NS	0	46	F	n/a	NPI-O/U	ART	+
H10	NS	0	32	M	12	HAD	No	-
H11	NS	0	53	M	4	Normal	HAART	+
H12	NS	0	50	M	15	NPI-O/U	ART	-
H13	NS	1	44	M	12	Normal	No	n/a
H14	NS	0	41	M	14	ANI	No	-
H15	NS	0	56	M	12	HAD	HAART	+
H16	NS	0	53	F	38	Normal	No	+
H17	NS	0	38	M	10	Normal	No	+
H18	NS	0	41	F	6	Normal	No	n/a
H19	NS	0	52	F	8	Normal	ART	+
H20	NS	0	39	M	7	ANI	ART	n/a
H21	NS	0	36	F	2	ANI	No	-
H22	NS	0	38	M	10	NPI-O/U	No	-
H23	NS	1	42	M	7	MND	HAART	-
H24	NS	1	34	F	15	Normal	HAART	-
H25	NS	0	40	M	5	MND	HAART	-
H26	NS	0	45	M	20	NPI-O/U	HAART	+
H27	NS	0	46	M	30	NPI-O/U	HAART	-
H28	NS	1	65	M	24	MND	HAART	-
H29	S	0	37	M	12	MND	No	+
H30	S	0	27	M	8	MND	HAART	+
H31	S	1	52	M	24	NPI-O/U	HAART	-
H32	S	0	60	M	46	ANI	HAART	+
H33	S	0	44	M	11	MND	No	+
H34	S	0	54	M	12	MND	HAART	-
H35	S	1	39	M	12	ANI	HAART	-
H36	S	0	36	M	13	MND	ART	+
H37	S	0	45	M	8	HAD	n/a	-
H38	S	0	39	M	48	MND	HAART	-
H39	S	0	47	M	12	Normal	HAART	-

Case	Sestrin-2 pattern ^a	p-Tau grade ^b	Age	Sex	PMI (h)	NC Dx ^c	ARV Rx	METH
H40	S	1	56	M	12	MND	HAART	–
H41	S	0	35	M	10	NPI-O/U	HAART	+
H42	S	0	59	M	12	n/a	HAART	–

Abbreviations: HIV, human immunodeficiency virus; p-Tau, phospho-Tau; PMI, postmortem interval; NC Dx, neurocognitive diagnosis; ARV Rx, antiretroviral treatment; HAART, highly active antiretroviral therapy regimens; ART, non-HAART antiretroviral regimens; METH, lifetime methamphetamine use; M, male; F, female; n/a, data not available; +, presence; –, absence.

^aSestrin-2 immunoreactivity in the left mid-frontal cortex of HIV cases is classified into three patterns: *neuropil* predominance (N), *neuropil and neuronal-soma* co-dominance (NS), and *neuronal-soma* predominance (S).

^bThe density of p-Tau-immunoreactive neuropil threads is graded as 0, 1, 2, and 3 (Alafuzoff et al. 2008).

^cHIV-associated neurocognitive disorders are classified into asymptomatic neurocognitive impairment (ANI), mild neurocognitive disorder (MND), and HIV-1-associated dementia (HAD) (Antinori et al. 2007), while cognitive impairments determined to be unrelated to HIV infection are assigned as neuropsychological impairment due to other or undetermined causes (NPI-O/U)

Table 2

Autopsy non-HIV controls and Alzheimer's disease cases

	Brain	Sestrin-2	p-Tau grade ^c	Age	Sex	PMI (h)
Control		Pattern ^a				
C1	RF	N	1	72	F	16
C2	RP	N	0	43	F	30
C3	RP	N	0	90	F	12
C4	LF	N	1	76	M	n/a
C5	LF	N	0	33	F	10
C6	RF	N	0	35	F	15
C7	RF	N	0	72	M	26
C8	LF	N	0	24	M	21
C9	RF	N	1	14	M	22
C10	LF	N	1	48	F	12
C11	LF	N	1	32	M	22
C12	LF	N	0	33	M	26
C13	LF	N	0	47	F	15
C14	LF	NS	1	55	F	3
C15	LF	NS	0	53	M	8
C16	LF	NS	1	68	n/a	3
C17	LF	NS	0	48	M	14
C18	LF	S	0	26	M	7
Alzheimer's disease		Neurofibrillary ^b				
A1	LF/RH	+/+	3/3	81	F	20
A2	LF/LH	+/+	3/3	75	F	7
A3	LF/LH	+/+	2/3	83	M	5
A4	LF/RH	+/+	3/3	69	M	24
A5	LF/LH	+/+	3/3	86	F	7
A6	RF/RH	+/+	3/3	90	M	13
A7	RF/LH	+/+	3/3	90	M	72
A8	LF/RH	+/+	3/3	72	F	16
A9	RF/LH	+/+	3/3	86	F	24
A10	RF/LH	+/+	2/3	85	F	22
A11	LF/RH	+/+	3/3	87	M	24
A12	RF/LH	+/+	3/3	69	F	15
A13	LF/RH	+/+	3/3	76	F	21
A14	LP/RH	+/+	3/3	89	M	15
A15	LF/LH	+/+	3/3	74	F	13
A16	RF/LH	+/+	3/3	89	F	4
A17	RF/LH	+/-	3/3	85	F	96
A18	LF/RH	-/+	2/3	97	F	4

	Brain	Sestrin-2	p-Tau grade ^c	Age	Sex	PMI (h)
A19	LF / LH	- / -	3 / 3	86	F	72

Abbreviations: HIV, human immunodeficiency virus; p-Tau, phospho-Tau; PMI, postmortem interval; RF, right mid-frontal; LF, left mid-frontal; RP, right parietal; LP, left parietal; RH, right hippocampus; LH, left hippocampus; M, male; F, female; n/a, data not available; +, presence; -, absence.

^aSestrin-2 immunoreactivity in the isocortex of non-HIV controls is classified into three patterns: *neuropil* predominance (N), *neuropil and neuronal-soma* co-dominance (NS), and *neuronal-soma* predominance (S).

^bSestrin-2-immunoreactive neurofibrillary lesions (i.e. neurofibrillary tangles and plaque-associated dystrophic neurites) in the isocortex and hippocampus, respectively, of each Alzheimer's disease brain.

^cThe density of p-Tau-immunoreactive neuropil threads is graded as 0, 1, 2, and 3 (Alafuzoff et al. 2008). In each Alzheimer's disease brain, p-Tau grades are shown for the isocortex and hippocampus, respectively